

Highly dispersive photonic crystal fiber for beamforming

Maggie Yihong Chen¹, Harish Subbaraman², & Ray T. Chen²

¹Omega Optics Inc, 10435 Burnet Rd, Austin, TX 78758

²Microelectronics Research Center, The University of Texas at Austin, Austin, TX 78758

ABSTRACT

In this paper, a highly dispersive pure silica photonic crystal fiber is designed and fabricated with maximum chromatic dispersion value of about -600 ps/(nm·km) around 1.55 μm wavelength region. This kind of a photonic crystal fiber structure is suitable for high dispersion application in photonic crystal fiber array based phased array antenna systems.

A four-element true-time delay module is constructed using the fabricated highly dispersive photonic crystal fibers. The true time delay value of 10.5m PCF is characterized to provide maximum delay of 31.3ps with 32nm optical wavelength tuning range, which is sufficient to scan from -45° to 45° for a 4-element PAA subarray having 1.3cm spacing. A multiple-beam optical beamformer is designed based on the fabricated highly dispersive photonic crystal fibers. The true-time delay beamformer can be programmed to continuously sweep the antenna aperture independently for multiple RF beams. Since the dispersion of the fabricated photonic crystal fibers is as high as -600 ps/nm·km at 1550 nm, compared to telecom SMF-28 that has a dispersion parameter of 18 ps/nm·km, the length of delay line is reduced by a factor of 33.

Keywords: Dispersion, photonic crystal fiber, phased-array antenna, beamforming

1. INTRODUCTION

Phased Array Antenna (PAA) systems have many advantages over mechanically-steered antenna arrays in terms of speed, sensitivity, and size [1]. However, most of phased array antenna radar architectures suffer from problems of being bulky, sensitive to electromagnetic interference (EMI), beam squint effect, and limited bandwidth due to the installation of large amount of electrical cables and microwave phase-shifting devices. Today's phased array radar technologies call for frequency independent beam steering, compact and light weight systems, large instantaneous bandwidth, and EMI free performance [2]. These features can be realized by using optical true time delay techniques (TTD). Furthermore, systems with TTD have the intrinsic capability of multi-beam operation due to the fact that the optical signals with different optical wavelengths can propagate through a fiber without interfering with each other, for which the widely used Dense Wavelength Division Multiplexing (DWDM) system is an illustrative example. Many optical schemes have been proposed to take advantages of a photonic feed for true-time delay (TTD), including acousto-optic (AO) integrated circuit technique [3], Fourier optics technique [4], bulky optics technique [5], dispersive fiber technique [6], fiber grating technique [7], and substrate guided wave technique [8]. Of these techniques, the dispersive fiber technique can reduce the size and weight of the overall system by a significant factor. Conventional systems use single mode fibers (SMF) as delay lines to implement the dispersive fiber technique. Since the dispersion value (D) of SMF is small (~ 18 ps/nm/km @1550nm), longer lengths of fiber are generally required to generate larger time delay values. One alternative to solve this problem is to use highly dispersive photonic crystal fibers (PCF), which can be designed to have very large dispersion values compared to a conventional SMF [9]. By using such highly dispersive photonic crystal fibers as delay lines, we can reduce the fiber length dramatically compared to conventional SMF based systems.

In this paper, we designed and simulated highly dispersive fibers. We construct a four element true-time delay module with the highly dispersive fibers and characterize the time delay values. A multiple-beam true time delay X-band

beamformer is designed using highly dispersive photonic crystal fibers as delay lines. In the designed system, the beamformer can simultaneously transmit multiple beams from different directions.

2. HIGHLY DISPERSIVE PHOTONIC CRYSTAL FIBER DESIGN

In our design, the dual concentric-core PCF structure is adopted to achieve high dispersion value. The mechanism of a dual concentric-core PCF is very similar to that of a directional coupler [10]. First, we introduce the coupled mode theory on the dual core PCFs [11]. The central core and the outer core behave like two parallel waveguides and the high dispersion is from the coupling between the two waveguides. By expanding the propagation constants, β , of the modes in the isolated waveguides around the phase matched frequency using Taylor's series, we get [10]

$$\beta_i(\omega) \approx \beta(\omega_p) + (\omega - \omega_p) \left. \frac{d\beta_i}{d\omega} \right|_{\omega=\omega_p} + \frac{(\omega - \omega_p)^2}{2} \left. \frac{d^2\beta_i}{d\omega^2} \right|_{\omega=\omega_p} \quad (1)$$

where $i = 1, 2$ represents the inner and the outer waveguide respectively and ω_p represents the phase matched frequency. From the coupled mode theory, we know that the coupling of the individual modes can generate two super-modes, whose propagation constants can be written as [10]

$$B_{+/-} = \frac{1}{2} \{ [\beta_1(\omega) + \beta_2(\omega)] \pm \sqrt{[\beta_1(\omega) - \beta_2(\omega)]^2 + 4\kappa^2} \} \quad (2)$$

where κ is the coupling constant between the two waveguides. We can insert Eq. (1) into Eq. (2) and differentiate the result twice with respect to angular frequency. Supposing that the two waveguides' $\left. \frac{d^2\beta}{d\omega^2} \right|_{\omega=\omega_p}$ are all very small

numbers (this term is mainly determined by the material dispersion of waveguide, and so it must be a very small term), we get the group velocity dispersion as

$$\frac{d^2B_{+/-}}{d\omega^2} = \pm \frac{1}{4\kappa} \left(\frac{d\beta_1}{d\omega} - \frac{d\beta_2}{d\omega} \right)^2 \times \left[\frac{(\omega - \omega_p)^2}{4\kappa^2} \left(\frac{d\beta_1}{d\omega} - \frac{d\beta_2}{d\omega} \right)^2 + 1 \right]^{-\frac{3}{2}} \quad (3)$$

The dispersion parameter is defined as

$$D = -\frac{\lambda}{c} \frac{d^2n_{eff}}{d\lambda^2} = -\frac{2\pi c}{\lambda^2} \frac{d^2B}{d\omega^2} \quad (4)$$

Using Eq. (3) and Eq. (4) we get

$$D = \mp \frac{\pi}{2c\kappa} \left(\frac{dn_1}{d\lambda} - \frac{dn_2}{d\lambda} \right)^2 \times \left[\frac{\pi^2}{\kappa^2} \frac{(\lambda - \lambda_p)^2}{\lambda_p^2} \left(\frac{dn_1}{d\lambda} - \frac{dn_2}{d\lambda} \right)^2 + 1 \right]^{-3/2} \quad (5)$$

From Eq. (5), we see that the dispersion value reaches its maximum value when λ is equal to λ_p and is given by

$$D_{Max} = \mp \frac{\pi}{2c\kappa} \left(\frac{dn_1}{d\lambda} - \frac{dn_2}{d\lambda} \right)^2 \quad (6)$$

From Eq. (6), we see that the dispersion value mainly depends on the coupling constant κ and the difference of $dn/d\lambda$ between the inner and the outer core.

The parameters of the fiber were carefully chosen to make the respective modes have a phase match at a wavelength (λ_p) close to 1.55 μm . At the phase match wavelength around 1.55 μm , the effect of varying the period (Λ) on $dn/d\lambda$ and coupling constant κ are carefully studied using fully vectorial plane wave expansion (PWE) method [12]. Since the PCF is not a perfect crystal without defects, a supercell of size 8 x 8, instead of a unit cell is implemented for periodic boundary conditions. From simulations we find that the period (Λ) plays a vital role in achieving broadband operation along with a very high dispersion value. By designing structures with very small periods, we can achieve very high dispersion-bandwidth products. However, it becomes very difficult to control the diameter of the air holes over such small dimensions. Simulations also show that any small deviation in the air hole diameters can totally change the dispersion curve in terms of magnitude and position. Therefore, the parameters need to be strictly controlled while drawing the fibers. This sets a limit on the manufacturability. Higher dispersion value requires smaller inner core diameter ($\sim 1.5 \mu\text{m}$), which makes the coupling from a standard single mode fiber to this fiber very difficult and lossy. With the designed microstructure of $\Lambda=3.5 \mu\text{m}$, $d_0=1.72 \mu\text{m}$, $d_1=1.45 \mu\text{m}$, $d_2=1.08 \mu\text{m}$, $d_3=0.86 \mu\text{m}$, $\Delta n_1/n=1.9\%$, and $\Delta n_2/n=1.3\%$, the schematic diagram showing the cross section is illustrated in Figure 1. The dispersion is $-600 \text{ ps/nm}\cdot\text{km}$ at 1550 nm, which is increased by 33 times compared to telecom SMF-28 that has a dispersion coefficient of 18 $\text{ps/nm}\cdot\text{km}$, and by 6 times compared to conventional DCF which has a dispersion coefficient of -100ps/nm/km .

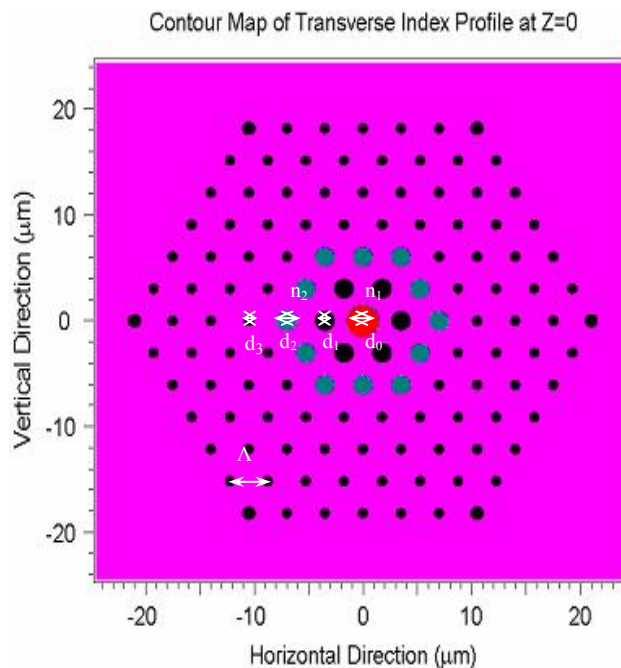


Fig. 1. Schematic diagram showing the cross section of the PCF.

3. HIGHLY DISPERSIVE PHOTONIC CRYSTAL FIBER CHARACTERIZATION

The scanning electron micrograph (SEM) of a fabricated PCF is shown in Figure 2. Between the inner silica core and outer silica core, there is one ring of air hole. The outer cladding is composed by four rings of air holes.

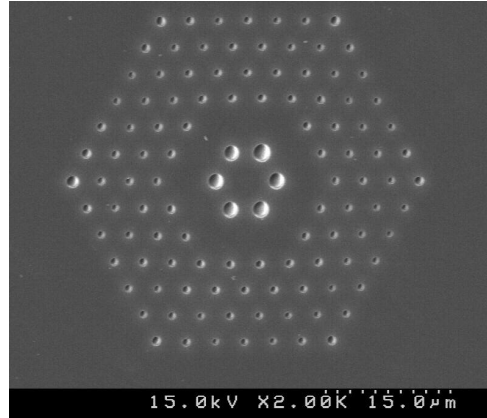


Fig. 2. Scanning Electron Micrograph (SEM) cross section of the PCF.

A four element true-time delay module is constructed with four PCF and SMF segments. The first element is 10.5m SMF; the second element is 7m SMF plus 3.5m PCF; the third element is 3.5m SMF plus 7m PCF; the fourth element is 10.5m PCF. The 1545nm wavelength is chosen as a reference for zero time delay. By tuning the wavelength from 1528 nm to 1560 nm, time delays ranging from -31.3 ps to 31.3 ps between any two adjacent delay lines are achieved. This is equivalent to scanning angles from -45° to 45° for a 4-element PAA subarray having 1.3cm spacing between adjacent elements. We measure the time delay from each delay line at 1550nm with 1545nm as the reference using a digital communication analyzer, which is shown in Fig.3. It is measured that 11.04ps delay interval is achieved with 5nm wavelength deviation, which agree with calculated delay value from the measured dispersion curve [13].

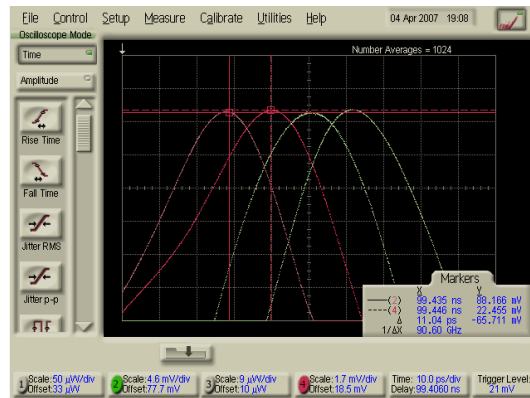


Fig. 3. Measured time delay of four PCF delay lines at 1550nm.

4. MULTIPLE BEAM TRANSMITTER DESIGN

The Simultaneous steering of multiple RF beams is very attractive for both military and commercial applications. Multiple-beam transmit/receive functions can be realized by allocating multiple wavelengths. Each wavelength represents a specific RF beam direction. Fig.4 shows a schematic drawing of the operation principle for optical beamformer architecture with an arbitrary number (M) of wavelengths feeding an N -element array antenna. For a single RF beam transmission, only one tunable laser is presented to provide optical carrier with wavelength λ_1 . The optical carrier is modulated with the RF signal using an electro-optic modulator (EOM). The modulated optical carrier feeds the photonic crystal fiber (PCF) based TTD module. The TTD module is to provide time delay for N -element PAA such that the steering angle can be continuously tuned by tuning the wavelength of the laser. After the pre-designated time delay within the delay modules, the N optical signals are converted into the corresponding electrical signals by N photodiodes as depicted in Fig.4. The electrical signals are then fed to the N -element phased array antenna head.

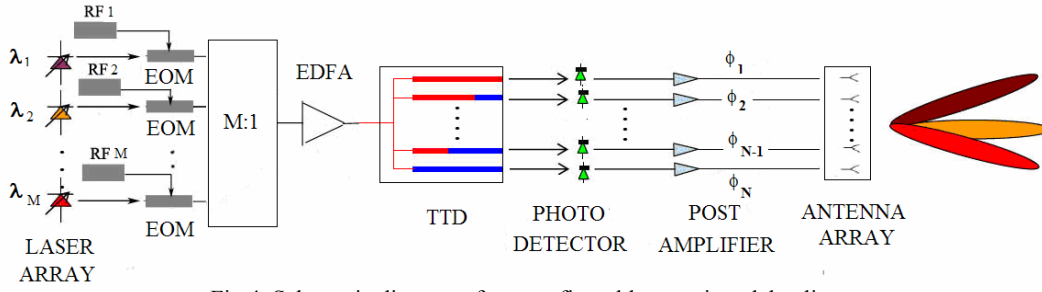


Fig.4. Schematic diagram of a reconfigurable true-time delay line.

The feeding links of each antenna element in Fig.4 is calibrated to have the same nominal group delay at wavelength λ_0 . When the optical wavelength is tuned from λ_0 to λ_i , the time delay t_i corresponding to the i^{th} element of the PAA is expressed as:

$$t_i = L_i \cdot \int_{\lambda_0}^{\lambda_i} D(\lambda) d\lambda, \quad i = 1, 2, \dots, N \quad (7)$$

where L_i is the length of PCF in the i^{th} delay line; and $D(\lambda)$ is the dispersion coefficient of the PCF at optical wavelength λ . The length difference of PCFs between adjacent delay lines is designed as $\Delta L = L_i - L_{i-1}$. Consequently, the time delay interval Δt between adjacent delay lines is:

$$\Delta t = \Delta L \cdot \int_{\lambda_0}^{\lambda_i} D(\lambda) d\lambda \quad (8)$$

The achievable steering angle for the RF beam is:

$$\theta = \arcsin \left(\frac{c \cdot \Delta L \cdot \int_{\lambda_2}^{\lambda_1} D(\lambda) d\lambda}{d} \right) \quad (9)$$

where d is the separation between adjacent antenna array elements. It is obvious from the above equation that the beam can be steered with the optical wavelength continuously.

In order to achieve multiple-beam independent operation, we simply need to employ multiple tunable lasers corresponding to the number of beams. In Fig.1, totally M tunable lasers are employed to generate M independently steered RF beams. Each optical carrier is modulated with an RF signal and then combined by a $1 \times M$ combiner. The modulated optical signals pass through a $1 \times N$ optical power splitter and fed to the PCF-based TTD module, which provides the following time delay matrix

$$t_{i,k} = \begin{matrix} & \begin{matrix} 1 & 2 & \dots & N \text{ (element number)} \end{matrix} \\ \begin{matrix} 1 \\ 2 \\ \vdots \\ M \end{matrix} & \begin{matrix} L_1 \cdot \int_{\lambda_0}^{\lambda_1} D(\lambda) d\lambda & L_2 \cdot \int_{\lambda_0}^{\lambda_2} D(\lambda) d\lambda & \dots & L_N \cdot \int_{\lambda_0}^{\lambda_1} D(\lambda) d\lambda \\ L_1 \cdot \int_{\lambda_0}^{\lambda_2} D(\lambda) d\lambda & L_2 \cdot \int_{\lambda_0}^{\lambda_2} D(\lambda) d\lambda & \dots & L_N \cdot \int_{\lambda_0}^{\lambda_2} D(\lambda) d\lambda \\ \vdots & \vdots & \ddots & \vdots \\ L_1 \cdot \int_{\lambda_0}^{\lambda_M} D(\lambda) d\lambda & L_2 \cdot \int_{\lambda_0}^{\lambda_M} D(\lambda) d\lambda & \dots & L_N \cdot \int_{\lambda_0}^{\lambda_M} D(\lambda) d\lambda \end{matrix} \end{matrix}$$

(Beam number)

where N is the element number and M is the RF beam number to be independently steered simultaneously. The first row in the matrix represents a time interval $\Delta L \cdot \int_{\lambda_0}^{\lambda_1} D(\lambda) d\lambda$, corresponding to steering angle at $\theta_1 = \arcsin \left(\frac{c \cdot \Delta L \cdot \int_{\lambda_2}^{\lambda_1} D(\lambda) d\lambda}{d} \right)$.

The second row in the matrix represents a time interval $\Delta L \cdot \int_{\lambda_0}^{\lambda_2} D(\lambda) d\lambda$, corresponding to steering angle at

$\theta_2 = \arcsin\left(\frac{c \cdot \Delta L \cdot \int_{\lambda_2}^{\lambda_2} D(\lambda) d\lambda}{d}\right)$. While the Mth row in the matrix represents a time interval $\Delta L \cdot \int_{\lambda_0}^{\lambda_M} D(\lambda) d\lambda$, corresponding to

steering angle at $\theta_M = \arcsin\left(\frac{c \cdot \Delta L \cdot \int_{\lambda_2}^{\lambda_M} D(\lambda) d\lambda}{d}\right)$. The multiple-beam transmitter can continuously steer multiple RF beams

with only N delay lines.

5. CONCLUSION

In conclusion, we present the design and simulation of highly dispersive PCFs. A multiple-beam optical beamformer based on highly dispersive photonic crystal fibers is designed. The true-time delay beamformer can be programmed to continuously sweep the antenna aperture independently for multiple RF beams. A four-element true-time delay module is constructed using the fabricated highly dispersive photonic crystal fibers. The true time delay performance of the TTD module is demonstrated. The true time delay values of 10.5m PCF are confirmed to provide maximum delay of 31.3ps with 32nm optical wavelength tuning range.

6. REFERENCES

1. C. A. Balanis, *Antenna theory: Analysis and design*, 3rd Edition, John Wiley & Sons, 2005.
2. W. Ng, A. A. Walston, G. L. Tangonan, J. J. Lee, I. L. Newberg, and N. Bernstein, "The first demonstration of an optically steered microwave phased array antenna using true-time-delay," *IEEE Journal of Lightwave Technology*, **9**, pp. 1124-1131, 1991.
3. L. H. Gesell, R. E. Feinleib, J. L. Lafuse, and T. M. Turpin, "Acousto-optic control of time delays for array beam steering", *Proc. of SPIE*, **2155**, pp. 194, 1994.
4. G. A. Koepf, "Optical processor for phased-array antenna beam formation", *Proc. Of SPIE*, Vol.477, pp. 75-81, 1984.
5. N. A. Riza, "Liquid crystal-based optical time delay control system for wideband phased arrays", *Proc. Of SPIE*, **1790**, 171, 1992.
6. D. T. K. Tong and M. C. Wu, "Multiwavelength Optically Controlled Phased-Array Antennas", *IEEE Trans. On Microwave and Tech*, **46**, No.1, pp. 108-115, 1998.
7. Molony A., Edge C., and Bennion I., "Fiber grating time delay element for phased array antennas," *Elec. Lett.*, **31**, pp. 1485-1486, 1995.
8. Yihong Chen, Ray T. Chen, "A fully Packaged True Time Delay Module for a K-band Phased Array Antenna System Demonstration", *IEEE. Photon. Technol. Lett*, **14**, pp.1175-1177, 2002.
9. Harish Subbaraman, Tao Ling, YongQiang Jiang, Maggie. Y. Chen, Peiyan Cao, and Ray T. Chen, "Design of a broadband highly dispersive pure silica photonic crystal fiber", *Applied Optics*, **46**, No. 16, pp. 3263-3268, 2007.
10. U. Peschel, T. Peschel, and F. Lederer, "A compact device for highly efficient dispersion compensation in fiber transmission," *Appl. Phys. Lett.* **67**, 2111-2113, 1995.
11. S. K. Varshney, T. Fujisawa, K. Saitoh, and M. Koshiba, "Design and analysis of a broadband dispersion compensating photonic crystal fiber Raman amplifier operating in S-band," *Opt. Express*. **14**, 3528-3540, 2006.
12. K. M. Ho, C. T. Chan, C. M. Soukoulis, "Existence of a Photonic Gap in Periodic Dielectric Structures," *Phy. Rev. Lett.* **65**, 3152-3155, 1990.
13. Y. Jiang, Z. Shi, B. Howley, X. Chen, M. Y. Chen, and R. T. Chen, "Delay Time Enhanced Photonic Crystal Fiber array for Wireless Communications using 2-D X-band Phased-Array Antennas," *Opt. Engineering*, **44**, 2005, 125001.